Optical Properties of Wurtzite GaN and ZnO Quantum Dots

Vladimir A. Fonoberov and Alexander A. Balandin
Nano-Device Laboratory, Department of Electrical Engineering,
University of California-Riverside, Riverside, California 92521, U.S.A.

ABSTRACT

We have investigated exciton states in wurtzite GaN/AlN and ZnO quantum dots. A strong piezoelectric field in GaN/AlN quantum dots is found to tilt conduction and valence bands, thus pushing the electron to the top and the hole to the bottom of the GaN/AlN quantum dot. As a result, the exciton ground state energy in GaN/AlN quantum dots with heights larger than 3 nm exhibits a red shift with respect to bulk GaN energy gap. It is shown that the radiative decay time in GaN/AlN quantum dots is large and increases from 0.3 ns for quantum dots with height 1.5 nm to 1.1×10^3 ns for the quantum dots with height 4.5 nm. On the contrary, the electron and the hole are not separated in ZnO quantum dots. Moreover, a relatively thick "dead layer" is formed near the surface of ZnO quantum dots. As a result, the radiative decay time in ZnO quantum dots is small and decreases from 73 ps for quantum dots with diameter 1.5 nm to 29 ps for the quantum dots with diameter 6 nm.

INTRODUCTION

Wurtzite GaN/AlN and ZnO quantum dots (QDs) have recently attracted attention as promising nanostructured materials for optoelectronic applications. Optical properties of QDs strongly depend on the QD size. Although the band gap energy for GaN and ZnO is nearly the same (about 3.5 eV), the optical properties of GaN/AlN and ZnO QDs are different. The main difference in the optical properties of these QDs comes from the presence of strong strain and piezoelectric fields in GaN/AlN QDs and absence of those fields in ZnO QDs (see Refs. [1-3]). In this paper we carry out a rigorous calculation of exciton states in both types of QDs. The results of our calculations are compared with available experimental data and the difference in the optical spectra of GaN/AlN and ZnO QDs is discussed.

THEORY

In order to calculate exciton states in wurtzite GaN/AlN QDs we use the theoretical model from Refs. [1-3]. The model allows us to takes into account the strain and piezoelectric fields present in the GaN/AlN QDs. It also explicitly includes degeneracy and anisotropy of conduction and valence bands. Since the radius of the region of electron and hole localizations in the considered GaN/AlN QDs is less than the exciton Bohr radius of bulk GaN (~ 2 nm), we first calculate separate electron and hole states in those QDs and then consider the electron-hole Coulomb interaction as a perturbation. The electrostatic piezoelectric potential $V_p(\mathbf{r})$, generated by the sum $\mathbf{P}(\mathbf{r})$ of the spontaneous and the strain-induced polarizations, is found by solving the Maxwell equation:

$$\nabla\cdot\left(\hat{\varepsilon}_{\text{stat}}(\mathbf{r})\nabla V_p(\mathbf{r})-4\pi\mathbf{P}(\mathbf{r})\right)=0,$$

where $\hat{\varepsilon}_{\text{stat}}(\mathbf{r})$ is the dielectric tensor. Electron states are found as the eigenstates of the one-band envelope-function equation with the following Hamiltonian

$$\hat{H}_e = \hat{H}_S(\mathbf{r}_e) + H_e^{(\varepsilon)}(\mathbf{r}_e) + E_c(\mathbf{r}_e) + eV_p(\mathbf{r}_e),$$

where $\hat{H}_S$ and $H_e^{(\varepsilon)}$ are the kinetic and strain-dependent parts of the electron Hamiltonian, correspondingly, E_c is the energy of unstrained conduction band edge, and e is the absolute value of electron charge. Hole states are found as the eigenstates of the six-band envelope-function equation with the following Hamiltonian

$$\hat{H}_h = \begin{pmatrix} \hat{H}_{XYZ}(\mathbf{r}_h) + H_h^{(\varepsilon)}(\mathbf{r}_h) & 0 \\ 0 & \hat{H}_{XYZ}(\mathbf{r}_h) + H_h^{(\varepsilon)}(\mathbf{r}_h) \end{pmatrix} + E_v(\mathbf{r}_h) + eV_p(\mathbf{r}_h) + H_{\text{so}}(\mathbf{r}_h),$$

where, $\hat{H}_{XYZ}$ is a 3×3 matrix of the kinetic part of the hole Hamiltonian (including the crystal-field splitting energy), $H_h^{(\varepsilon)}$ is a 3×3 matrix of the strain-dependent part of the hole Hamiltonian, E_v is the energy of the unstrained valence band edge, and H_{so} is the Hamiltonian of spin-orbit interaction.

In order to calculate exciton states in wurtzite ZnO QDs in water we use the same electron and hole Hamiltonians as those for wurtzite GaN/AlN QDs, but without the strain and piezoelectric contributions. The exciton Bohr radius of bulk ZnO (~ 0.9 nm) is smaller than the size of considered QDs, therefore we cannot consider the electron-hole Coulomb interaction as a perturbation for ZnO QDs and one has to solve the six-dimensional exciton problem numerically. The following Hamiltonian is used to calculate the exciton states in ZnO QDs:

$$\hat{H}_{exc} = \left[\hat{H}_e + V_{\text{s-a}}(\mathbf{r}_e)\right] - \left[\hat{H}_h - V_{\text{s-a}}(\mathbf{r}_h)\right] + V_{\text{int}}(\mathbf{r}_e, \mathbf{r}_h).$$

Since dielectric constants in ZnO QD and the exterior medium are different the Coulomb potential energy of the electron-hole system is represented by the sum of the electron-hole interaction energy $V_{\text{int}}(\mathbf{r}_e, \mathbf{r}_h)$ and electron and hole self-interaction energies $V_{\text{s-a}}(\mathbf{r}_e)$ and $V_{\text{s-a}}(\mathbf{r}_h)$ defined in Ref. [4]. By making use of the axial symmetry of exciton wave functions along the *c*-axis in wurtzite ZnO, we can reduce the exciton problem to a five-dimensional one. Due to the axial symmetry of the exciton problem, the *z*-component of the exciton angular momentum *M* is a good quantum number. Therefore, one can represent the exciton wave function in the form:

$$\Psi_M(\mathbf{r}_e, \mathbf{r}_h) = \frac{1}{2\pi} \sum_{m=-\infty}^{\infty} \begin{pmatrix} \Psi_{X+iY}^{M,m}(\rho_e, z_e; \rho_h, z_h)\, e^{i(m-1)\varphi} \times e^{i(M-1)\Phi} \\ \Psi_{Z}^{M,m}(\rho_e, z_e; \rho_h, z_h)\, e^{im\varphi} \times e^{iM\Phi} \\ \Psi_{X-iY}^{M,m}(\rho_e, z_e; \rho_h, z_h)\, e^{i(m+1)\varphi} \times e^{i(M+1)\Phi} \end{pmatrix}.$$

The small spin-orbit interaction and the penetration of the exciton wave function outside the QD are neglected for ZnO QDs.

For both GaN/AlN and ZnO QDs, the oscillator strength f of an exciton state with energy E_{exc} and envelope wave function $\Psi_{\text{exc}}(\mathbf{r}_e, \mathbf{r}_h)$ is calculated as

$$f = \frac{E_P}{E_{\text{exc}}} \left| \int_V \Psi_{\text{exc}}^{(\alpha)}(\mathbf{r}, \mathbf{r})\, d\mathbf{r} \right|^2,$$

where E_P is the Kane energy and α denotes the component of the wave function, which is active for a given polarization. Using the oscillator strength, one can find the exciton radiative lifetime:

$$\tau = 2\pi\varepsilon_0 m_0 c^3 \hbar^2 \Big/ \sqrt{\varepsilon}\, e^2 E_{\text{exc}}^2 f.$$

RESULTS

Using the theory presented in the previous section one can calculate the optical spectra of wurtzite GaN/AlN and ZnO QDs as a function of QD size. Self-assembled GaN/AlN QDs have the shape of a truncated hexagonal pyramid on a wetting layer. According to Ref. [5], the geometry of a GaN/AlN QD with height H can be described by the thickness of the wetting layer $w = 0.5$ nm, QD bottom diameter $D_B = 5(H - w)$, and QD top diameter $D_T = H - w$. According to Ref. [6], colloidal ZnO QDs have nearly spherical shape. Material parameters used in our calculations are taken from Ref. [2] for GaN/AlN QDs and from Ref. [7] for ZnO QDs. To compute exciton states, strain tensors, and piezoelectric potentials we use simple numerical models described in Ref. [2]. In the following, z-axis of the coordinate system is chosen to be parallel to the c-axis of wurtzite GaN and ZnO nanocrystals.

It is seen in Fig. 1 that the piezoelectric potential in the GaN/AlN QD tilts conduction and valence band edges along the z-axis in such a way that it creates a potential well for the electron near the QD top and for the hole in the wetting layer near the QD bottom. Figure 2 shows the distribution of the piezoelectric potential in the GaN/AlN QD. The results of our numerical calculation of the exciton ground state energy levels for wurtzite GaN/AlN and ZnO/water QDs

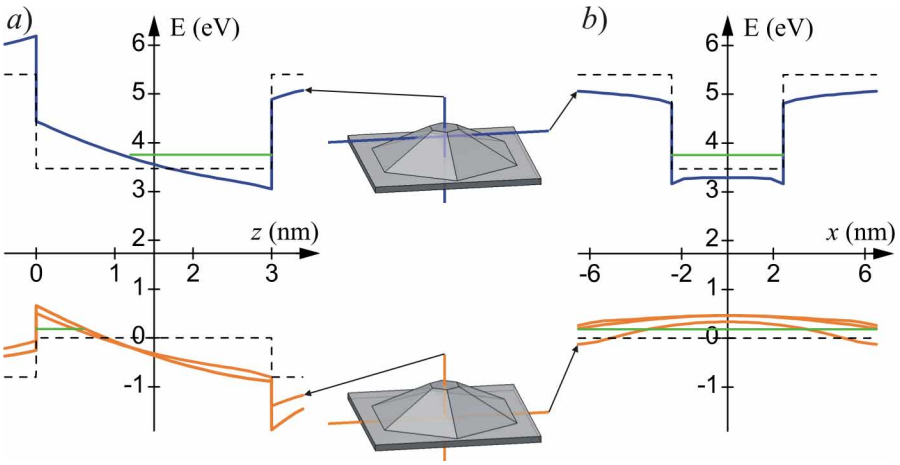

Fig. 1. Conduction and valence band edges along z-axis (a) and along x-axis (b) for GaN/AlN QD with height 3 nm (solid lines). The valence band edge is split due to the strain and crystal fields. Dashed lines show the conduction and valence band edges in the absence of strain and piezoelectric fields. Green lines show positions of electron and hole ground state energies.

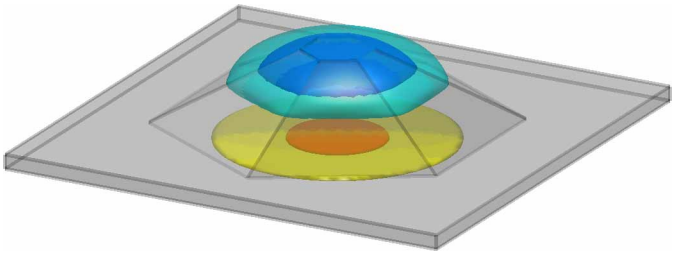

Fig. 2. Piezoelectric potential in the GaN/AlN QD with height 3 nm.

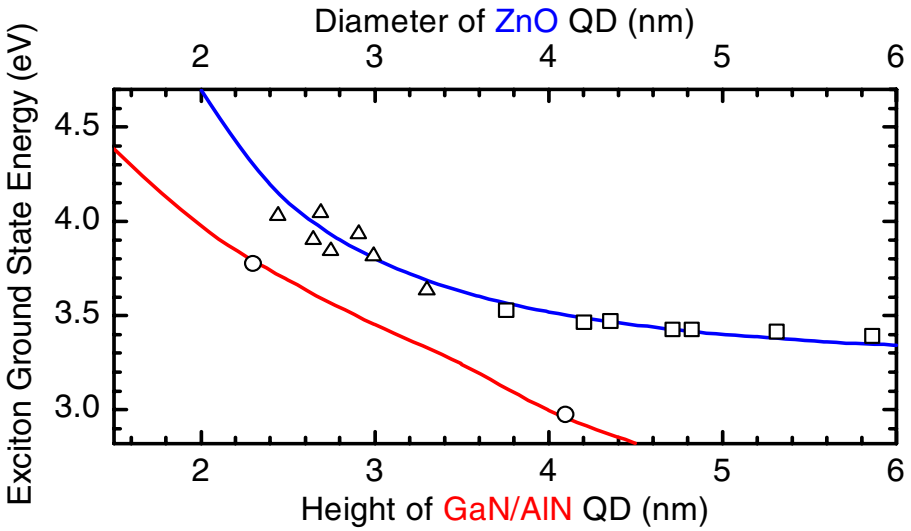

Fig. 3. Exciton ground state energy as a function of QD size for GaN/AlN QDs (red line) and for ZnO QDs in water (blue line). Circles (Ref. [5]), boxes (Ref. [8]), and triangles (Ref. [9]) are experimental data points.

are shown in Fig. 3 as a function of the QD height or QD diameter. As seen, our calculations are in excellent agreement with the experimental data of Refs. [5, 8, 9]. It is found that the exciton ground state energy drops below the bulk wurtzite GaN energy gap for GaN/AlN QDs higher than 3 nm. Such a huge red-shift of the exciton ground state energy with respect to the bulk wurtzite GaN energy gap is attributed to the strong piezoelectric field in GaN/AlN QDs.

It is seen from Fig. 4 that the electron in GaN/AlN QDs is pushed to the QD top, while the hole is localized in the wetting layer, near to the QD bottom. One can also notice that the increase of the GaN/AlN QD's size by a factor of two leads to a much smaller increase in the effective volume occupied by the electrons and holes. Figure 5 shows that, due to the intrinsic anisotropy of wurtzite ZnO, the exciton's center of mass in ZnO QDs is prolate along the *z*-axis.

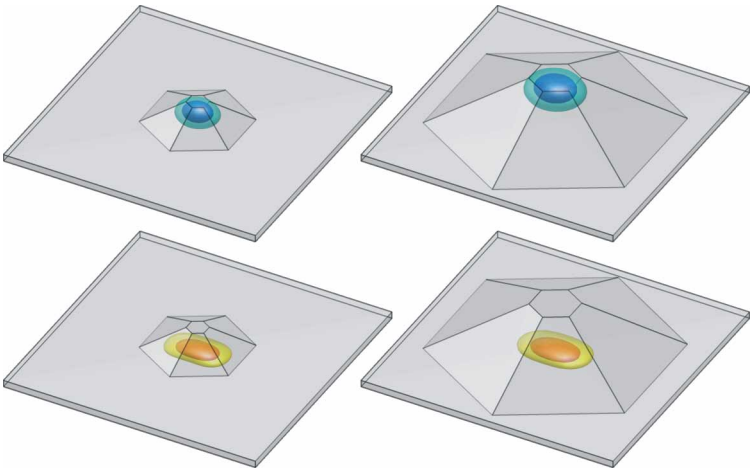

Fig. 4. Electron (top) and hole (bottom) ground state densities in GaN/AlN QDs with heights 2 nm and 4 nm.

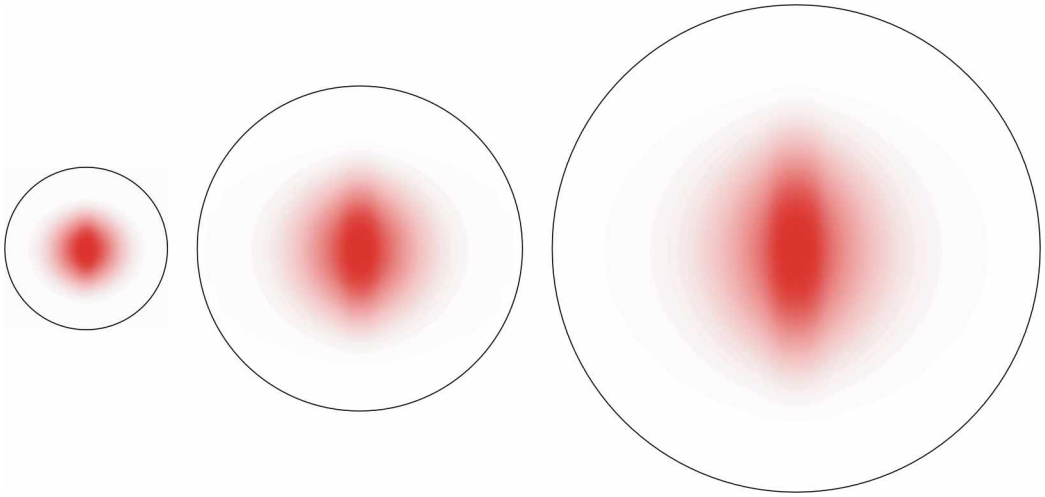

Fig. 5. Exciton wave function with equal electron and hole coordinates for ZnO QDs with diameters 2 nm, 4 nm, and 6 nm. The z-axis is vertical.

The exciton Bohr radius of bulk ZnO is less than the radius of considered ZnO QDs; therefore, the electron and hole motion around their center of mass prevents the center of mass from reaching QD surface, thus, forming a so-called "dead layer" near the QD surface. It is seen from Fig. 5 that the "dead layer" increases with QD size.

Finally, Fig. 6 shows the exciton radiative lifetimes for GaN/AlN and ZnO QDs as a function of QD size. The radiative lifetime of the red-shifted transitions in GaN/AlN QDs ($H > 3$ nm) is large and increases almost exponentially from 6.6 ns for QDs with height 3 nm to 1100 ns for QDs with height 4.5 nm in a very good agreement with the experimental data from Ref. [10]. The rapid increase of the radiative lifetime in GaN/AlN QDs is caused by the rapid

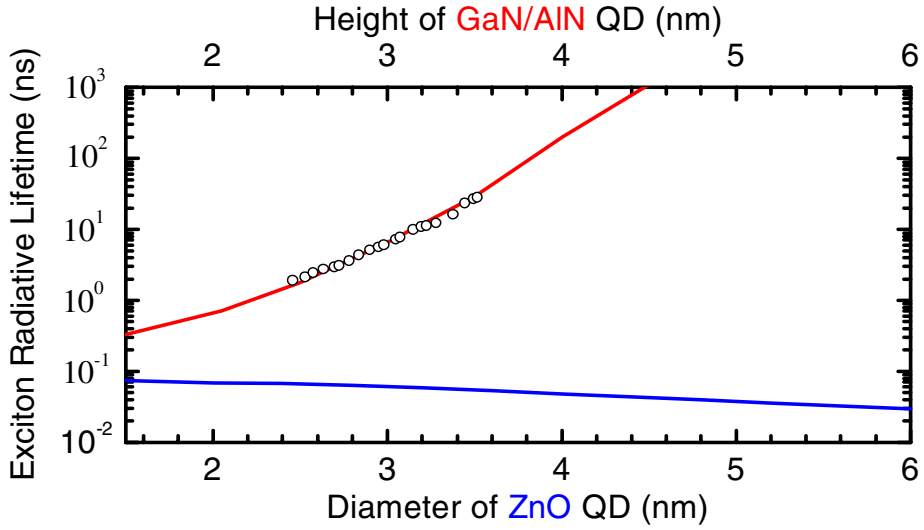

Fig. 6. Exciton radiative lifetime as a function of QD size for GaN/AlN QDs (red line) and for ZnO QDs in water (blue line). Circles are experimental data points from Ref. [10].

decrease of the electron-hole overlap with increasing the QD height. To the best of our knowledge, no measurements of the exciton radiative lifetime in ZnO QDs have been carried out. It is seen from Fig. 6 that the radiative lifetime in ZnO QDs is small and decreases from 73 ps for QDs with diameter 1.5 nm to 29 ps for the QDs with diameter 6 nm. For the ZnO QD with diameter 5 nm we get the lifetime of about 38 ps, in agreement with the conclusion of Ref. [6].

CONCLUSIONS

We have shown that there is a major difference in the optical properties of wurtzite GaN/AlN and ZnO QDs. While the exciton radiative lifetime of GaN/AlN QDs is large and increases with QD height, the exciton radiative lifetime of ZnO QDs is shown to be small and decrease with QD diameter.

ACKNOWLEDGEMENTS

This work is supported in part by the NSF-NATO 2003 award to V.A.F., ONR Young Investigator Award N00014-02-1-0352 to A.A.B., Microelectronics Advanced Research Corporation (MARCO), and DMEA/DARPA CNID program A01809-23103-44.

REFERENCES

1. V. A. Fonoberov, E. P. Pokatilov, and A. A. Balandin, J. Nanosci. Nanotechnol. **3**, 253 (2003).
2. V. A. Fonoberov and A. A. Balandin, J. Appl. Phys. **94**, 7178 (2003).
3. V. A. Fonoberov and A. A. Balandin, J. Vac. Sci. Technol. B, in press (2004).
4. V. A. Fonoberov, E. P. Pokatilov, and A. A. Balandin, Phys. Rev. B **66**, 085310 (2002).
5. F. Widmann, J. Simon, B. Daudin, G. Feuillet, J. L. Rouviere, N. T. Pelekanos, and G. Fishman, Phys. Rev. B **58**, R15989 (1998).
6. D. W. Bahnemann, C. Kormann, and M. R. Hoffmann, J. Phys. Chem. **91**, 3789 (1987).
7. W. R. L. Lambrecht, A. V. Rodina, S. Limpijumnong, B. Segall, and B. K. Meyer, Phys. Rev. B **65**, 075207 (2002).
8. E. A. Muelenkamp, J. Phys. Chem. B **102**, 5566 (1998).
9. A. Wood, M. Giersig, M. Hilgendorff, A. Vilas-Campos, L. M. Liz-Marzan, and P. Mulvaney, Aust. J. Chem. **56**, 1051 (2003).
10. J. Simon, N. T. Pelekanos, C. Adelmann, E. Martinez-Guerrero, R. Andre, B. Daudin, L. S. Dang, and H. Mariette, Phys. Rev. B **68**, 035312 (2003).